Evaluation of Correlation Between Surface Diaphragm Electromyography and Airflow Using Fixed Sample Entropy in Healthy Subjects

Xiaoyu Gu, Shuai Ren, Yan Shi, Xiao Li, Zixuan Guo, Xuelin Zhao, Zhihao Mao, Maolin Cai, and Fei Xie

***Abstract*— In clinic, the acquisition of airflow with nasal prongs, masks, thermistor to monitor respiratory function is more uncomfortable and inconvenience than surface diaphragm electromyography (EMGdi) using electrode pads. The EMGdi with strong electrocardiograph (ECG) interference affect the extraction of its characteristic information. In this work, surface EMGdi and airflow signals of 20 subjects were collected under 5 incremental inspiratory threshold loading protocols from quiet breathing to maximum forced breathing. First, we filtered out the ECG interference in EMGdi based on the combination of stationary wavelet transform and the positioning of ECG to obtain pure EMGdi ($EMGdi_p$). Second, the Spearman's rank correlation coefficients between EMGdi and $EMGdi_p$ quantified by time series fixed sample entropy (fSampEn), root mean square (RMS), and envelope were compared to verify the robustness of the fSampEn to ECG. A comparative analysis of correlation between fSampEn of EMGdi and inspiratory airflow and the correlation between envelope of $EMGdi_p$ ($EMGdi_e$) and inspiratory airflow found that there was no significant difference between the two, indicating the feasibility of using fSampEn to predict airflow. Moreover, fSampEn of EMGdi was used as characteristic parameter to build a quantitative relationship with the airflow by polynomial regression analysis. Mean coefficient of determination of all subjects in any breathing state is greater than 0.88. Finally, nonlinear programming method was used to solve a universal fitting coefficient between fSampEn of EMGdi and airflow for each subject to further evaluate the possibility of using surface EMGdi to monitor and control respiratory activity.**

***Index Terms*— Diaphragm electromyography, airflow, stationary wavelet transform, fixed sample entropy, polynomial regression analysis.**

Manuscript received August 16, 2021; revised November 23, 2021 and December 29, 2021; accepted January 14, 2022. Date of publication January 18, 2022; date of current version February 1, 2022. This work was supported in part by the National Natural Science Foundation of China under Grant 52005015, in part by the Outstanding Young Scientists in Beijing under Grant BJJWZYJH01201910006021, in part by the National Key Research and Development Project under Grant 2019YFC0121702 and Grant 2019YFC0121703, in part by the Military Medicine Innovation Research Project of PLA General Hospital under Grant CX19030, in part by the Key Projects of Translational Medicine in PLA General Hospital under Grant 2018TM-03, in part by the Clinical Research Support Project of PLA General Hospital under Grant 2019XXJSYX13, and in part by the Medical Big Data Research and Development Project of PLA General Hospital under Grant 2019XXMBD-013. *(Corresponding authors: Yan Shi; Fei Xie.)*

This work involved human subjects or animals in its research. Approval of all ethical and experimental procedures and protocols was granted by the Biology and Medical Ethics Committee of Beihang University under Reference No. BM20210155.

Xiaoyu Gu is with the School of Biology and Medical Engineering, Beihang University, Beijing 100191, China (e-mail: guxiaoyu@buaa.edu.cn).

Shuai Ren is with the School of Automation, Beijing Institute of Technology, Beijing 100811, China, and also with the School of Automation Science and Electrical Engineering, Beihang University, Beijing 100191, China (e-mail: renshuai@bit.edu.cn).

Yan Shi and Maolin Cai are with the School of Automation Science and Electrical Engineering, Beihang University, Beijing 100191, China (e-mail: shiyan@buaa.edu.cn; caimaolin@buaa.edu.cn).

Xiao Li is with the Department of Rehabilitation, The Fourth Medical Center of PLA General Hospital, Beijing 100048, China (e-mail: yueerli1985@126.com).

Zixuan Guo and Xuelin Zhao are with the Department of Orthopedics, The Fourth Medical Center of PLA General Hospital, Beijing 100048, China (e-mail: gzx301@126.com; zxl_199013@163.com).

Zhihao Mao is with the Department of Neurosurgery, Xintai Hospital of Traditional Chinese Medicine, Shandong 271200, China (e-mail: mzhabcd567@163.com).

Fei Xie is with the Department of Pulmonary and Critical Care Medicine, Chinese PLA General Hospital, Beijing 100853, China (e-mail: xiefei0522@163.com).

Digital Object Identifier 10.1109/TNSRE.2022.3144412

I. Introduction

THE surface electromyography signal (EMG) is an electrical signal transmitted to the surface of the skin caused by the change of action potential when the muscle under the skin contracts. Although the time-domain waveform of the EMG signal can reflect the activity and characteristics of the muscle, it is chaotic [1]. It is usually necessary to extract meaningful information of the EMG signal through feature extraction. Root mean square (RMS) is the most commonly used feature extraction method to obtain the amplitude of muscle contraction, and its value can be used to determine the performance of certain muscles [2], [3].

The diaphragm is the most important respiratory muscle [4]. Its electromyography signal (EMGdi) produced during breathing reflects important physiological information of the respiratory system, and is an important basis for the diagnosis of respiratory diseases, such as chronic obstructive pulmonary disease (COPD) and asthma [5]. Compared with inspiratory flow and inspiratory pressure, EMGdi is the most effective method to assess neural respiratory drive (NRD), especially for patients with COPD [5], [6]. The acquisition of EMGdi signal is classified into invasive and body surface detection [5]. Surface electrode acquisition method has been used in clinical respiratory monitoring for its non-invasive, convenient and cheap advantages [7]. However, the surface EMGdi is a micro-electric signal, and it is affected by power frequency

interference [8], motion artifact [9], EMG of other respiratory muscles [10] and electrocardiographic (ECG) signal [11] during the acquisition process. The amplitude of the ECG is much higher than EMGdi and its main frequency band overlaps with the EMGdi [12], which has an adverse effect on the evaluation of EMGdi amplitude using RMS.

Several studies divided into two ways have shown how to filter out the interference of the ECG signal in the EMGdi. One is to increase the collection of the ECG signal and use it as a reference input to filter out the interference of the ECG signal by using shear substitution [13], adaptive noise cancellation (ANC) [14] and event synchronization cancellation (ESC) [15]. The other is to directly filter the ECG signal through stationary wavelet transform [11], mathematical morphology [16], and non-linearly scaled wavelets [17] on the EMGdi without ECG acquisition. Nevertheless, these studies focused on the filtering effect of the ECG in EMGdi, and did not perform further feature extraction and analysis on it.

Recently, a new method called fixed sample entropy (fSampEn), effectively weakening the interference of the ECG, has been proposed to assess respiratory muscle function from EMGdi [18], [19]. SampEn is an improved complexity measurement method based on approximate entropy [20]. It is robust to signals with impulsive noises, and can calculate a stable entropy value based on less data (1000-5000 points) [20]. Based on the SampEn, the value of the fSampEn is calculated through a fixed tolerance value. In [18], it is an effective method to use the fSampEn calculating the EMGdi to evaluate the NRD. In practice, computer-simulated EMGdi with and without ECG cannot truly reflect the actual collected EMGdi. The robustness of fSampEn to ECG interference should be confirmed based on the collected EMGdi.

As another important physiological signal reflecting the human breathing state, the respiratory airflow signal is often used in sleep monitoring [21] and ventilator triggering and control technology [22]. The measurement methods of airflow including nasal prongs, mask, thermistor are effective and reliable [23]. These methods involve varying degrees of contact with the human body. Nasal intubation requires a special catheter to be inserted into the trachea through the nose. In order to prevent the leakage of gas from affecting the measurement accuracy, the mask needs to be fastened to the face. The thermistor detects the airflow requires the thermistor to be placed in the nostril. From a clinical point of view, these detection methods are uncomfortable for the human, especially for infants and children, which will make them uneasy or even intolerable. It is significant to explore monitoring schemes for airflow to improve comfort and convenience in acquisition.

The aim of this work was to establish a quantitative correlation between airflow and surface EMGdi to assess the possibility of monitoring and controlling respiratory activity with surface EMGdi. First, we filtered out the ECG interference in EMGdi based on stationary wavelet transform. Second, by calculating the correlation between fSampEn, RMS and envelope of the EMGdi, the influence of the ECG in EMGdi was analyzed. Finally, on the basis of analyzing the correlation between the airflow, fSampEn and envelope, we proposed a method for quantitative evaluation between fSampEn and airflow.

II. Materials and Methods

A. Data Acquisition

The test subjects for the acquisition of physiological signals were 20 adults (10 males and 10 females, age: 25.3 $\pm$ 2.74 years old, weight: 66.35 $\pm$ 14.19kg, height: 170.15 $\pm$ 9.10cm) with no heart, lung and nervous system diseases. Before participating in the experiment, all subjects simply understood the process and purpose of the experiment, then signed the informed consent form. The Biology and Medical Ethics Committee of Beihang University (reference number BM20210155) and human subjects have approved these data collection.

The physiological signal (EMGdi and airflow) acquisition system was composed of hardware, software and a subject. The EMGdi was acquired by the physiological signal amplification module (FE234, Quad Bio Amp, ADInstruments, Sydney, Australia) with high performance differential amplifiers. Then the amplified EMGdi was recorded by the physiological recorder (PL3516, PowerLab 16/35, ADInstruments, Sydney, Australia) and transmitted to the PC software (Lab Chart 8, ADInstruments, Sydney, Australia) for reading, displaying and processing. The right diaphragm of the experimental subject was selected to obtain the EMGdi, which required a pair of measuring electrodes and a reference ground electrode. A pair of electrodes (positive electrode and negative electrode, spacing: 20mm) were placed separately at the intersection of the anterior axillary line and the sixth and eighth intercostals, with the positive electrode above the negative electrode [24]. The reference ground electrode was on the xiphoid process of the chest wall. After finding the electrode location, the scrub (Nuprep Skin Prep Gel, Weaver and Company, Aurora, USA) was used to rub the skin sufficiently cleaned with alcohol to reduce the skin/electrode impedance [24]. The disposable button-type body surface electrodes (diameter: 50mm, diameter contact with skin: 10mm, AC resistance: $\leq$3kΩ (10Hz), Heal Force, ShangHai, China) with hydrogel Ag/AgCl for sensing and viscous element were chosen to record the surface EMGdi.

The signal transmission wire that collected EMGdi connected to the electrode pads were glued and fixed on the skin surface with medical tape to reduce the artifacts of breathing movement. The sampling rate of the EMGdi signals in the LabChart software were set to 2000Hz [18], [24], and the filter bandwidth to 10-1000Hz. During the EMGdi signals collection process, the subject sit on a chair with his hands on knees and quietly received breathing instructions from the instrument operator. In addition, a key point in the experiment was to avoid verbal communication with the subject to keep the environment quiet and avoid interference.

Subjects in the experiment needed to complete 5 different breathing tasks, including Quiet breathing, Forced breathing I, Forced breathing II, Forced breathing III and Forced breathing IV. During data collection process, the respiratory rate of each breathing task was 15 times per minute. For

each subject, we first collected the inspiratory airflow for 90s and obtained average peak inspiratory airflow (af_1) in Quiet breathing state of the specified inhalation time and expiration time. Secondly, continuous 90s of breathing airflow under the state of maximum forced breathing (Forced breathing IV) was acquired to get the average peak of inspiratory airflow (af_5). The other three peaks of inspiratory airflow (Forced breathing I, Forced breathing II, Forced breathing IV) were superimposed on the basis of the previous breathing task with a difference of 25% of $(af_5 - af_1)$. The collection time for each breathing task was 90s and the subject rested for 5 minutes after completing it. During the acquisition process, the subjects needed to keep their eyes fixed on computer screen (LabChart) with visual feedback to control breathing time, and peak point of inspiratory airflow. According to the degree of breathing effort, the EMGdi and airflow of five different breathing exercises were recorded. The airflow of different breathing modes were measured by the gas mass flow sensor (Bilateral measurements, Range: −300L/min-300L/min, CAFS4000B series, Consensic, USA). The physiological signal recorder obtained the output voltage value of the sensor and displayed it on LabChart. The airflow sensor connected to a ventilator tube with a mouthpiece was fixed on an adjustable height tripod. In order to prevent the airflow out of the nasal cavity from affecting the measurement accuracy during the test, a nose clip was required to tighten the nasal cavity. Moreover, subjects needed to perform appropriate exercises to prevent airflow from leaking out of the mouth before test. The sampling rate of the airflow was the same as the EMGdi, and the LabChart recorded both signals at the same time. All data was collected during one visit. Continuous 60s EMGdi signals and airflow signals were used for calculation and analysis in resluts. Fig. 1 depicts the collected airflow signals (a) and EMGdi signals (b) of a healthy subject in five different breathing states for intercepting three breathing cycles. The processing of all recorded data was performed in MATLAB (v. R2019b, Natick, MA, USA).

B. Processing of EMGdi and Airflow

1) Estimation of Respiratory Cycle: A moving average filter was used to smooth the measured airflow signal, and its window width was 1399. The calculation of the respiratory airflow period was based on the zero-crossing criterion [24], [25]. It meant that airflow greater than the zero threshold was the inhalation phase, opposite was the exhalation phase. The intersection of the respiratory airflow and the zero threshold could be defined as the starting point of inspiration or respiration. The airflow signals of three breathing cycles in five breathing states of a subject were separately intercepted shown in Fig. 1.

2) Filtering of ECG Interference in EMGdi Signal: After using a 3th Chebyshev Type I filter with a cut-off frequency of 15-400HZ (passband attenuation: 3db, stopband attenuation: 15db) to preprocess collected EMGdi signal, the remaining signals were mainly QRS complexes of ECG with the characteristics of larger magnitude and concentrated distribution [11]. ECG in EMGdi signal was filtered by combining ECG interference location and wavelet threshold filtering [11], [26]. The position of ECG and the range of ECG interference was based on the characteristics of wavelet correlation coefficient. After thresholding the wavelet coefficients in the range of ECG interference, the reconstructed EMGdi signals would effectively filter out the ECG. The steps of using discrete stationary wavelet transform to filter out ECG in EMGdi were as follows.

a) Stationary wavelet decomposition: We defined EMGdi as S and the stationary wavelet decomposition formula of it was expressed as follows.

$$\begin{cases} \mathrm{a}_{i+1} = H^{[i]} a_i \\ d_{i+1} = G^{[i]} a_i \end{cases} \tag{1}$$

where, $\mathrm{a}_0 = \mathrm{S}$, a_{i+1} is the approximate coefficients, d_{i+1} is the detail coefficient, $H^{[i]}$, $G^{[i]}$ are the low-pass filter and high-pass filter coefficients respectively. The corresponding signal reconstruction formula is expressed as follows.

$$a_i = R_\varepsilon(a_i, \mathrm{d}_i) \tag{2}$$

where R_ε is refactoring the average operator.

According to the sampling frequency of the EMGdi (2000Hz) and the frequency of the ECG signal (0-50Hz), a 5-scale wavelet decomposition was performed on the EMGdi to obtain approximate coefficients and detail coefficients. The wavelet coefficient of each layer is represented by *Wx(i, j)*.

Where, x is the approximate coefficient or the detail coefficient, expressed by a or d, i is the wavelet coefficient of the i-th layer, j is the abscissa of the wavelet coefficient.

b) Location of ECG signal position: The square of the low-frequency coefficient ($coef(j) = |Wa(5, j)|^2$) was used to distinguish the EMGdi from the ECG interference [27]. The expression of ECG peak position (*Pos(j)*) detection to determine edge of ECG interference peak can be written as follows.

$$coef(j) > k \times \sum_{j=1}^{n} coef(j)/n \tag{3}$$

where, n is the length of the EMGdi, k is the threshold proportional constant, the value is 20-40. If the coefficient *coef(j)* is greater than k times its average value ($th = k \times \sum_{j=1}^{n} coef(j)/n$), then point j is considered to be near the ECG peak. Second we found the position point where the position point j corresponds to the maximum value of the wavelet coefficient is the ECG peak position.

c) Wavelet threshold denoising and wavelet reconstruction: The threshold is selected according to the Donoho algorithm [28], which is determined by the wavelet transform coefficient $W_x(i, j)$ and the expression is as follows.

$$\lambda = \sqrt{2 \ln N} median(|W_x(i, j)|)/0.6745 \tag{4}$$

where N is the length of the signal.

The peak position of the ECG signal ($p_{loc}(j)$) determine the average cycle length of the ECG (T_{ecg}). The interference interval before and after the ECG peak can be expressed as $[p_{loc}(j) - 0.24 \times T_{ecg},\ p_{loc}(j) + 0.16 \times T_{ecg}]$ [27].

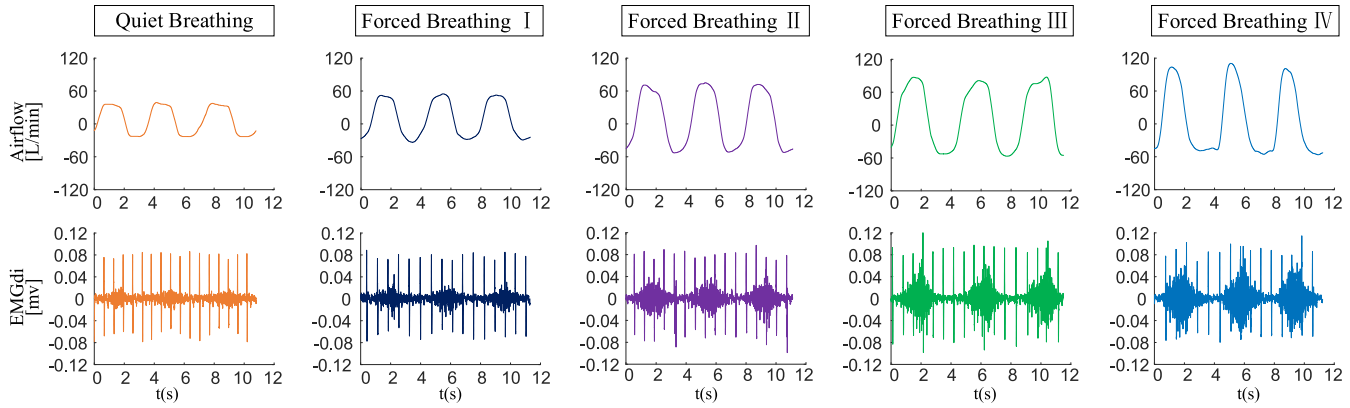

Fig. 1. The collected airflow signals (a) and EMGdi signals (b) of a healthy subject in five different breathing states for intercepting three breathing cycles. The five different breathing states refer to Quiet breathing and four breathing states (Forced Breathing I, Forced Breathing II, Forced Breathing III and Forced Breathing IV) that gradually increase the degree of exertion.

The 'inverse' hard threshold filtering [29] of the ECG signal can be expressed as

$$\overline{W}_x(i,j) = \begin{cases} W_x(x,j) & |W_x(i,j)| < \lambda \\ 0 & |W_x(i,j)| \geq \lambda \end{cases} \tag{5}$$

where, $\overline{W}_x(i,j)$ is the processed wavelet coefficient.

After the wavelet coefficients are processed, the wavelet reconstruction is performed to obtain the final signal after noise reduction ($EMGdi_p$).

C. Quantification of EMGdi

1) Fixed Sample Entropy and RMS: The sample entropy, proposed by Richman and Moorman, is a time series complexity measurement method [20]. It has strong anti-noise ability and consistency, and can obtain a stable entropy value using fewer data segments [20]. The lower signal sample entropy means the higher sequence self-similarity and lower sequence complexity. Fixed sample entropy (fSampEn) was developed based on the sample entropy algorithm, which was used to weaken the influence of the ECG noise in EMGdi signal. For an EMGdi with a section length of N, m-dimensional vectors (X_i, X_j, $i, j \leq$ N-m) were reconstructed. Maximum value of the distance between vector X_i and vector X_j marked as d_{ij} was calculated. Then for the similarity tolerance r, we counted the number of d_{ij} less than r as C, and calculate the ratio of it to the total number of vectors (N-m), so as to calculate the average of all vectors (A). Also the vector dimension to m + 1 was changed and we repeated the above steps to get B. The value of sample entropy was expressed as

$$SampEn(m,r,N) = -\ln\left(\frac{A^m(r)}{B^m(r)}\right) \tag{6}$$

Three main parameters needed to be determined in the calculation of sample entropy were the time series length (N), the vector dimension (m), and the similarity tolerance(r) respectively [30].

fSampEn was calculated based on the moving window and the fixed similarity tolerance r value in each window by using MATLAB. We used fSampEn to separately evaluate EMGdi (with ECG) and pure EMGdi without ECG ($EMGdi_p$) in different breathing states. The time length of the moving window was 1s and the overlap rate was 90%. On the basis of the previous study [24], m value was taken as 1. r value was set as 0.3 times the standard deviation of EMGdi (with ECG) and $EMGdi_p$ for each subject in 5 different breathing state.

The RMS of the EMGdi and $EMGdi_p$ were also calculated using a moving window. The length of the moving window and the overlap rate were 1s and 90% respectively.

2) Envelope of EMGdi Signal Without ECG: Previous studies [31] have shown that the envelope of the EMG signal can reflect the characteristics of different actions, and is smoother and more stable than the original signal. The pure EMGdi without ECG ($EMGdi_p$) signal in different breathing states was processed by a FIR high-pass filter with a cut-off frequency of 30 Hz and underwent full-wave rectification [32]. Then a low-pass FIR filter with a cut-off frequency of 2.5 Hz was used to implement envelope detection [7]. Finally, we used the sliding median filter method to obtain the smooth envelope of EMGdi without ECG ($EMGdi_e$).

D. Prediction of Respiratory Airflow

The fSampEn of EMGdi with 1-s moving window was used to predict the respiratory airflow based on polynomial fitting method. The amplitude of EMGdi increases during inhalation, but has no change during exhalation. Therefore, the fSampEn (fs) was used to predict the airflow (af_p) in the inhalation phase. In polynomial fitting, a higher order means a better fit between data points. Taking into account the characteristics of airflow and fSampEn and the accuracy of the calculation, a fifth-order polynomial was applied to predict the airflow. The relationship of them can be expressed as

$$af_p = f(fs) = \sum c_i fs^i \tag{7}$$

where, af_p and fs are respectively the airflow and fSampEn of EMGdi during the inhalation phase of each breathing state for all subjects, c_i is the fitting coefficient, $i = 0, 1, 2, 3, 4, 5$.

The nonlinear programming method was used to solve the same fitting coefficient of a subject in 5 breathing states. For

a subject in inhalation phase of each breathing state, initial values and peak points of fSampEn of the EMGdi signal (fs) and actual airflow (af_a) were extracted. The 5th order polynomial fitting relationship between fs and af_a were established respectively. Therefore, 10 fitting constraint relations were constructed. The objective function is the minimum sum of the difference between the predicted airflow (af_p) and actual value (af_a). The onset of the inspiratory airflow of each subject in each breathing state were zero. However, the corresponding initial values of fSampEn of EMGdi were different and not zero. Setting onset of sample entropy of surface EMG to zreo is a common method in the detection of the starting point of the EMG signal [33]. Therefore, we shift the corresponding fSampEn curve downward in inspiratory phase to make the onset value of fSampEn of EMGdi zero. The airflow and fSampEn of EMGdi of a breathing cycle in the inhalation phase under 5 different breathing states for a subject was used to calculate a fitting coefficient. The mathematical model for solving a single fitting coefficient of a subject in five breathing states were described as

$$\begin{cases} \min g(c_i) = \min \sum_{10} (af_p - af_a)^2 \\ \qquad\quad = \min \sum_{j=1}^{5} (\sum_{i=0}^{5} c_i fs(j)^i - af_a(j))^2 \\ s.t.\ af_a(j) = \sum_{i=0}^{5} c_i fs(j)^i \quad (j = 1, 2, \cdots, 10) \end{cases} \tag{8}$$

where, $g(c_i)$ is the objective function, af_p is the predicted airflow, af_a is the actual measured airflow, $fs(j)$ is initial value of fSampEn of EMGdi signal at onset of inhalation ($j = 1, 2, \ldots, 5$) and peak value of fSampEn of the EMGdi during inhalation ($j = 6, 7, \ldots, 10$) after the fSampEn of EMGdi in the inhalation phase minus its onset value for a subject in 5 breathing states. Sequential quadratic programming (SQP) algorithm was used to solve the fitting coefficients (c_i) in MATLAB. The upper and lower limits of coefficients ($[-10e+08, 10e+08]$) in the solver were adjusted to obtain a fitting coefficient for a subject in 5 breathing state.

E. Statistical Analysis Method

The correlation coefficient was used to assess the consistency between recorded data. Since the Lilliefors test judged that not all recorded signals obey a normal distribution, we used Spearman's rank correlation coefficient (ρ) to evaluate the correlation between two sets of parameters. The absolute value of the correlation coefficient (ρ) reflects the strength of the correlation [34], where very weak correlation for 0.0-0.19, weak correlation for 0.20-0.39, moderate correlation for 0.40-0.59, strong correlation for 0.60-0.79, very strong correlation for 0.80-1.00.

The correlation analysis method was used to analyze the parameters mainly include (1) fSampEn of EMGdi and $EMGdi_p$, (2) RMS of EMGdi and $EMGdi_p$, (3) $EMGdi_e$ and fSampEn of EMGdi, (4) $EMGdi_e$ and fSampEn of $EMGdi_p$, (5) RMS of EMGdi (EMGdi and $EMGdi_p$), (6) airflow and fSampEn of EMGdi (or $EMGdi_e$). Significant differences (p) between the fSampEn, breathing airflow, $EMGdi_e$ and RMS were analyzed by using the Mann-Whitney U test. If the p -value is less than 0.05, it can be considered that the correlation coefficients have statistically significant difference.

III. Results

A. Evaluation of Airflow and EMGdi in Different Breathing Status

Fig.2 illustrates (a) the $EMGdi_p$, (b) the $EMGdi_e$, and calculation of (c) fSampEn and (d) RMS for EMGdi (blue line) and $EMGdi_p$ (red line) in 5 different levels of breathing effort for a subject of 3 consecutive breathing cycles. In view of time-domain waveform of $EMGdi_p$, it was found that the ECG signal interference in EMGdi has been effectively filtered out. The amplitude of the $EMGdi_p$, $EMGdi_e$, fSampEn and RMS increases with the raise in the degree of breathing effort. Comparing the fSampEn values in 1-s moving window before and after filtering out the ECG signal, it can be obtained that although the numerical values are different, the waveform shapes of the two are basically the same. The ECG signal has a strong influence on the RMS value of the EMGdi signals in the moving window. The waveform and value of the RMS of EMGdi with and without ECG interference are completely different. After filtering out the ECG signal with higher amplitude, the value of RMS and fSampEn of $EMGdi_p$ have opposite trends. RMS values become smaller, and the fSampEn values increases.

Furthermore, the value of $EMGdi_p$ in the time domain diagram increase significantly during inhalation, and its value remains unchanged and close to zero during exhalation. The $EMGdi_e$, fSampEn, and RMS waveforms of $EMGdi_p$ seem extremely similar and are consistent with the breathing movement.

B. Assessment of the Respiratory Characteristics of All Subjects in Different Breathing States

In order to clarify the differences in the respiratory characteristics of all tested subjects, statistical calculation of the respiratory parameters (respiratory cycle, inspiratory time, and $EMGdi_e$) of them was implemented. Average breathing cycle values range from 3.8157s to 3.9283s in different breathing (Quiet breathing: 3.8277 $\pm$ 0.2919s, Forced breathing I:3.8157 $\pm$ 0.3488s, Forced breathing II: 3.8607 $\pm$ 0.2891s, Forced breathing III:3.9242 $\pm$ 0.3653s, Forced breathing IV:3.9283 $\pm$ 0.3531s). Mean inspiratory time values range from 1.9246s to 2.0909s at different levels of breathing effort (Quiet breathing: 2.0821 $\pm$ 0.2649s, Forced breathing I:2.0909 $\pm$ 0.1822s, Forced breathing II: 2.0716 $\pm$ 0.2092s, Forced breathing III:2.0241 $\pm$ 0.2515s, Forced breathing IV:1.9246 $\pm$ 0.2377s).

Fig.3 (a) and (b) respectively show mean and standard deviation of maximum airflow and $EMGdi_e$ of all subjects' continuous 60s breathing under different exertion levels (B1: Quiet breathing, B2: Forced breathing I, B3: Forced breathing II, B4: Forced breathing III, B5: Forced breathing IV). It was observed that as the degree of breathing effort rises, the maximum airflow and the envelope of $EMGdi_e$ signal also increases. Mean maximum airflow

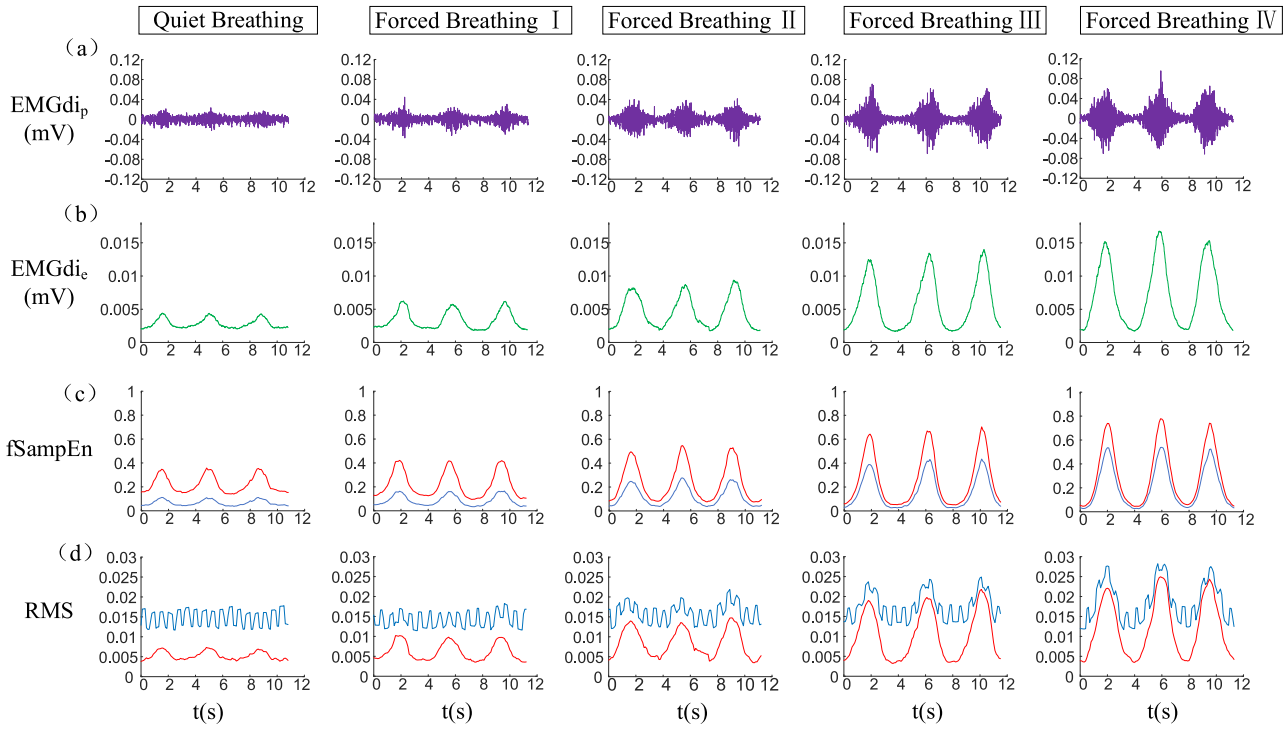

Fig. 2. Time series of envelope, fSampEn, and RMS of EMGdi before and after filtering out ECG interference in a subject shown in Fig. 2. (a) pure EMGdi without ECG signal (EMGdi$_p$), (b) Envelope of EMGdi without ECG (EMGdi$_e$), (c) fSampEn and (d) RMS of EMGdi$_p$ (red line) and EMGdi (blue line). EMGdi$_p$: pure EMGdi without ECG interference, EMGdi: EMGdi with ECG interference, EMGdi$_e$: envelope of EMGdi without ECG interference.

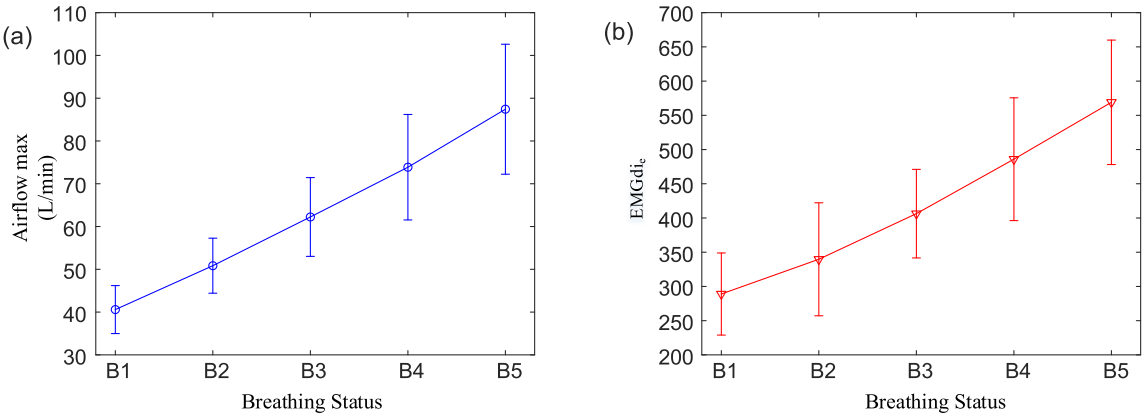

Fig. 3. (a) Maximum respiratory airflow and (b) envelope of EMGdi without ECG (EMGdi$_e$) under gradually increasing forced breathing (B1: quiet breathing, B2: Forced Breathing I, B3: Forced Breathing II, B4: Forced Breathing III, B5:Forced Breathing IV). The data points represent mean and standard deviation of the maximum respiratory airflow and envelope of EMGdi$_p$ (EMGdi$_e$) of all subjects under different respiratory tasks for 60s. EMGdi$_e$: envelope of pure EMGdi without ECG.

values range from 40.5941 L/min to 87.4308 L/min with gradual increases in respiration (Quiet breathing: 40.5941 ± 5.6088 L/min, Forced breathing I: 50.8494 ± 6.4299 L/min, Forced breathing II: 62.2392 ± 9.2074 L/min, Forced breathing III: 73.8775 ± 12.3292 L/min, Forced breathing IV: 87.4308 ± 15.1972 L/min). Average EMGdi$_e$ values range from 288.9516 to 569.0587 in 5 types of breathing with increasing exertion (Quiet breathing: 288.9516 ± 59.9717, Forced breathing I: 339.6872 ± 82.5625, Forced breathing II: 406.3561 ± 64.6795, Forced breathing III: 485.9518 ± 89.6925, Forced breathing IV: 569.0587 ± 90.8824). The differences in the respiratory characteristics of different subjects did not disturb the sorting of respiratory airflow and EMGdi signal values under different forced breathing states.

C. Influence of ECG on EMGdi

Fig. 4(a) explains the mean and standard deviation of ρ values between fSampEn and RMS of calculation about EMGdi and EMGdi$_p$ for all subjects completing gradually increasing forced breathing tasks. The value of ρ was used to appraise the influence of ECG signal on the fSampEn and RMS. It was

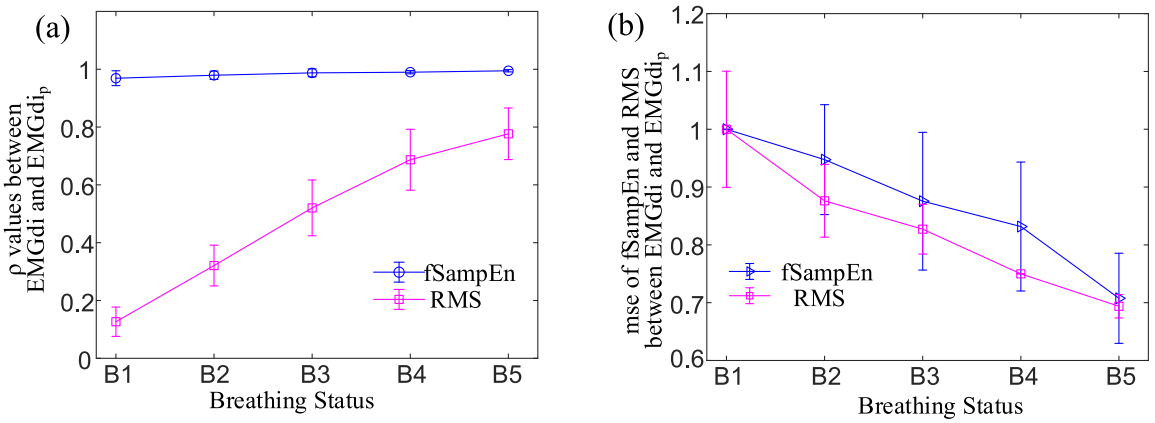

Fig. 4. (a) Mean and standard deviation of spearman's correlation coefficient (ρ) of fSampEn and RMS and (b) MSE of fSampEn and RMS over EMGdi and $EMGdi_p$ in all subjects under gradually increasing forced breathing (B1: quiet breathing, B2:Forced Breathing I, B3:Forced Breathing II, B4: Forced Breathing III, B5:Forced Breathing IV). $EMGdi_p$: pure EMGdi without ECG.

TABLE I
MEAN SPEARMAN'S CORRELATION COEFFICIENT (ρ) BETWEEN FSAMPEN AND $EMGDI_e$ IN ALL SUBJECTS UNDER GRADUALLY INCREASING FORCED BREATHING

Breathing state	Mean ρ between fSampEn of EMGdi and $EMGdi_e$	p	Mean ρ of fSampEn of $EMGdi_p$ and $EMGdi_e$	p
Quiet breathing	0.8387	P<0.001	0.8172	P<0.001
Forced breathing Ⅰ	0.8854	P<0.001	0.8761	P<0.001
Forced breathing Ⅱ	0.9198	P<0.001	0.9135	P<0.001
Forced breathing Ⅲ	0.9226	P<0.001	0.9152	P<0.001
Forced breathing Ⅳ	0.9367	P<0.001	0.9360	P<0.001
Mean and standard deviation	0.9006±0.0353	P<0.001	0.8916±0.0419	P<0.001

$EMGdi_e$: envelope of pure EMGdi without ECG, $EMGdi_p$: pure EMGdi without ECG interference

TABLE II
MEAN SPEARMAN'S CORRELATION COEFFICIENT (ρ) BETWEEN RMS AND $EMGDI_e$ IN ALL SUBJECTS UNDER GRADUALLY INCREASING FORCED BREATHING

Breathing state	Mean ρ between RMS of EMGdi and $EMGdi_e$	p	Mean ρ of RMS of $EMGdi_p$ and $EMGdi_e$	p
Quiet breathing	0.2327	0.0345	0.8532	P<0.001
Forced breathing Ⅰ	0.3711	0.0276	0.8756	P<0.001
Forced breathing Ⅱ	0.4388	0.0002	0.9125	P<0.001
Forced breathing Ⅲ	0.5549	0.0034	0.9349	P<0.001
Forced breathing Ⅳ	0.6464	P<0.001	0.9404	P<0.001
Mean and standard deviation	0.4487±0.1436	0.0164±0.0148	0.9033±0.0338	P<0.001

$EMGdi_e$: envelope of pure EMGdi without ECG, $EMGdi_p$: pure EMGdi without ECG interference

observed that with the increase in the amplitude of the EMG signal, the ρ values also increase accordingly. Compared with fSampEn, the correlation ρ values of RMS between EMGdi and $EMGdi_p$ changes significantly. It means that ECG signals interfere with the evaluation of the RMS of EMGdi and the effect decrease as the amplitude of EMGdi increases. The increase of breathing effort has no obvious effect on the correlation ρ value of fSampEn before and after filtering ECG of EMGdi. In all breathing states, the correlation value ρ obtained by fSampEn was observed to be greater than 0.9. At quiet breathing state (average maximum airflow: 40.5941 ± 5.6088 L/min), the weak correlation value of the RMS is 0.2514 ± 0.1240, while the fSampEn shows a very strong correlation value of 0.9740 ± 0.0277. At forced breathing IV state (average maximum airflow: 87.4308 ± 15.1972 L/min), a strong correlation (0.7195 ± 0.1180) of RMS was observed, and a very strong correlation (0.9964 ± 0.0033) of fSampEn was found. The correlation values of fSampEn and RMS under all breathing states are statistically significant ($p < 0.05$). Fig.4 (b) represents normalised mean squared error (MSE) of fSampEn and RMS of EMGdi and $EMGdi_p$. MSE was utilized to further evaluate the changes in fSampEn and RMS before and after the ECG interference was filtered out. MSE decreases with the increase of EMGdi amplitude, which means that the influence of ECG on the quantitative evaluation of EMGdi is inseparable from its amplitude. The normalised MSE of

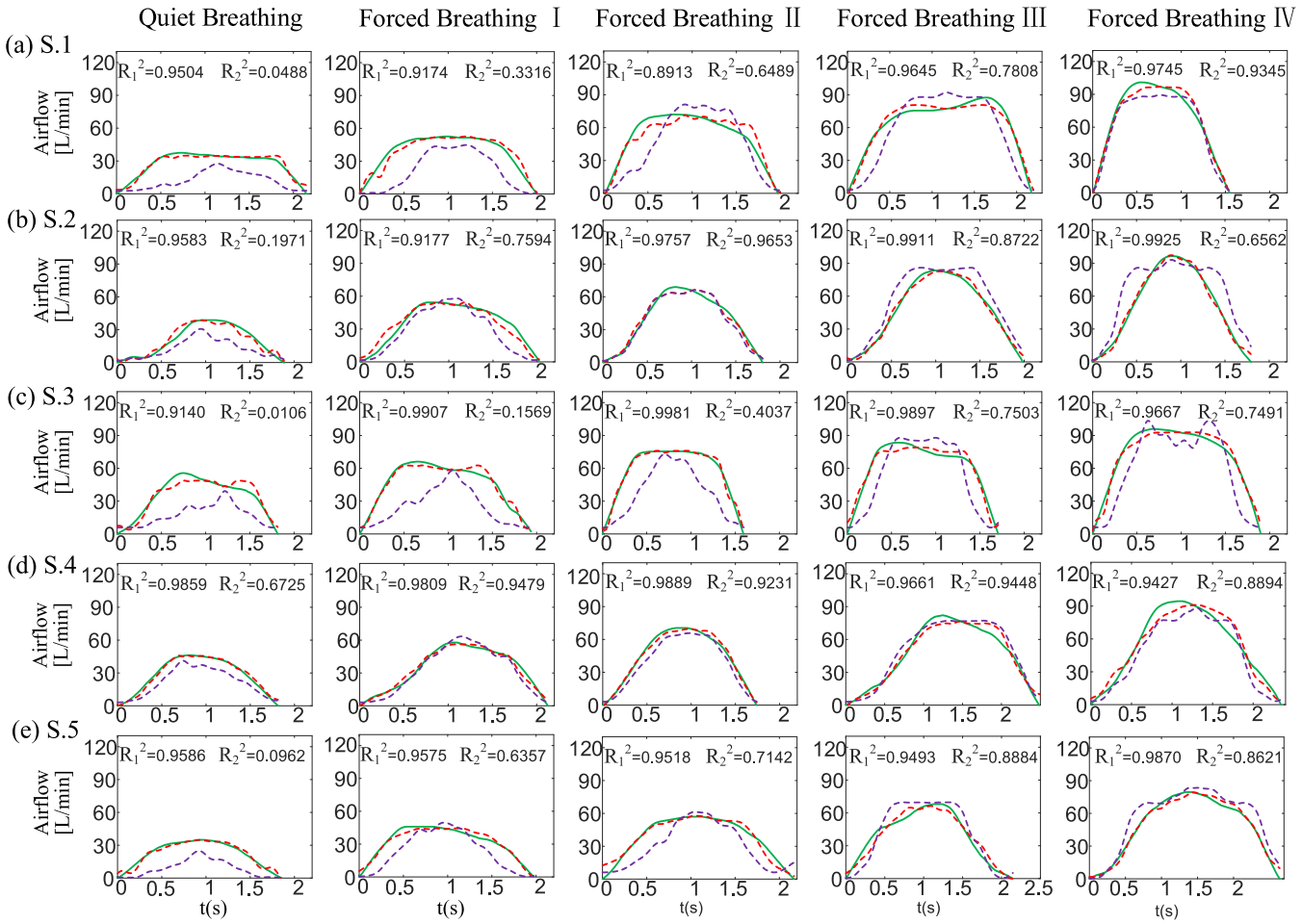

Fig. 5. The predicted airflow by multiple fitting coefficients (red dotted line) and a fitting coefficient (purple dotted line) and actual airflow (green solid line) in 5 breathing state (Quiet breathing, Forced breathing I, Forced breathing II, Forced breathing III, and Forced breathing IV respectively) in 5 subjects of (a) S.1, (b) S.2, (c) S.3, (d) S.4 and (e) S.5. The actual airflow in each breathing state is taken from the inspiratory airflow in 5 subjects. The predicted airflow is realized by time series fSampEn of EMGdi using polynomial curve fitting method. Coefficient of determination (R^2) was used to evaluate the goodness of fit of the model. R_1^2 is with differ ent fitting coefficients at different breathing state for a subject. R_2^2 is with a fitting coefficient at different breathing state for a subject.

fSampEn before and after the ECG is filtered is higher than the RMS.

Table I shows mean Spearman's correlation coefficient (ρ) between fSampEn of EMGdi (with and without ECG), and $EMGdi_e$ in all subjects for any breathing task. The correlation between fSampEn of EMGdi (or $EMGdi_p$) and $EMGdi_e$ in any breathing task show a very strong correlation ($\rho > 0.8$). All correlations are statistically significant ($p < 0.001$). It means that fSampEn in the moving window is consistent with the change of the EMGdi during breathing, and can effectively interfere with the ECG.

Table II indicates mean Spearman's correlation coefficient (ρ) between RMS of EMGdi (with and without ECG) and $EMGdi_e$ in all subjects for any breathing task. In either respiratory status, the correlation coefficient (ρ) between the RMS of EMGdi and $EMGdi_e$ after filtering interference of ECG is significantly greater than that before filtering. A weak correlation was observed between RMS of EMGdi and $EMGdi_e$ at quiet breathing state, and mean deviation correlation coefficient value in all subjects for only 0.2327. However, after filtering out the ECG, mean and standard deviation of the correlation coefficient for very strong correlation reached 0.8532. The correlation coefficient value of the RMS of EMGdi and $EMGdi_e$ increase with the increase of the degree of breathing effort. The change of the correlation coefficient between RMS of $EMGdi_p$ and $EMGdi_e$ is not evident, but its mean value greater than 0.80 of very strong correlation and corresponding correlations are statistically significant ($p < 0.001$).

D. Evaluation of Predicting Inspiratory Airflow Using fSampEn of EMGdi

Before using fSampEn of the EMGdi to estimate the airflow, the correlation between $EMGdi_e$ and the inspiratory airflow, and correlation between fSampEn of the EMGdi and the inspiratory airflow were evaluated. 15 consecutive inspiratory airflows, fSampEn of EMGdi and $EMGdi_e$ of any breathing state of each subject were used for correlation calculation.

Table III shows the Spearman's correlation coefficient values (ρ) in all subjects under gradually increasing forced breathing. The $EMGdi_e$ has a good correlation with the

TABLE III
SPEARMAN'S CORRELATION COEFFICIENT (ρ) BETWEEN INSPIRATORY AIRFLOW AND FSAMPEN OF EMGDI (OR $EMGdi_e$) IN ALL SUBJECTS UNDER GRADUALLY INCREASING FORCED BREATHING

Breathing state	Mean ρ between inspiratory airflow and fSampEn of EMGdi	p	Mean ρ between inspiratory airflow and $EMGdi_e$	p
Quiet breathing	0.8003	P<0.001	0.8013	P<0.001
Forced breathing Ⅰ	0.8054	P<0.001	0.8149	P<0.001
Forced breathing Ⅱ	0.8524	P<0.001	0.8016	P<0.001
Forced breathing Ⅲ	0.8428	P<0.001	0.8250	P<0.001
Forced breathing Ⅳ	0.8614	P<0.001	0.8237	P<0.001
Mean and standard deviation	0.8325±0.0249	P<0.001	0.8133±0.0102	P<0.001

$EMGdi_e$: envelope of pure EMGdi without ECG interference.

TABLE IV
DIFFERENT FITTING COEFFICIENTS AT DIFFERENT BREATHING STATE TO FIT AIRFLOW BASED ON FSAMPEN OF EMGDI FOR 5 SUBJECTS

Breathing state		Quiet breathing	Forced breathing I	Forced breathing II	Forced breathing III	Forced breathing IV
S.1	c_5	-6.60E+08	6.62E+07	-4.10E+06	3.60E+04	9.22E+04
	c_4	1.12E+08	-1.77E+07	2.19E+06	-5.00E+04	-6.44E+04
	c_3	-6.44E+06	1.85E+06	-3.90E+05	2.82E+04	1.32E+04
	c_2	1.25E+05	-9.78E+04	2.24E+04	-8.36E+03	-1.57E+03
	c_1	5.84E+02	2.97E+03	5.30E+02	1.30E+03	6.03E+02
	c_0	3.76E+00	9.09E-01	-1.57E+00	-1.96E+00	-1.67E+00
S.2	c_5	1.51E+08	-7.64E+07	-1.76E+07	-8.81E+05	4.99E+04
	c_4	-1.24E+07	1.69E+07	6.06E+06	6.11E+05	1.47E+02
	c_3	-6.77E+05	-1.25E+06	-7.76E+05	-1.61E+05	-1.29E+04
	c_2	7.80E+04	3.24E+04	4.44E+04	1.83E+04	3.70E+03
	c_1	-9.23E+02	5.18E+02	-3.87E+02	-3.32E+02	4.07E+01
	c_0	3.25E+00	3.64E+00	1.80E+00	3.51E+00	1.33E+00
S.3	c_5	3.88E+08	-7.08E+07	-1.94E+06	-1.72E+06	-1.29E+04
	c_4	1.80E+07	1.60E+07	8.45E+05	1.03E+06	-3.91E+04
	c_3	-3.12E+06	-1.26E+06	-1.12E+05	-2.11E+05	2.65E+04
	c_2	6.90E+04	3.41E+04	2.36E+02	1.47E+04	-4.21E+03
	c_1	9.43E+02	6.33E+02	1.07E+03	4.40E+02	3.33E+02
	c_0	4.50E+00	3.98E+00	-2.66E-02	-3.17E+00	5.19E-01
S.4	c_5	-7.71E+07	2.13E+06	5.72E+06	1.28E+06	-2.25E+05
	c_4	1.70E+07	-1.06E+06	-1.96E+06	-7.66E+05	2.01E+05
	c_3	-1.40E+06	1.56E+05	2.17E+05	1.53E+05	-6.26E+04
	c_2	5.26E+04	-8.58E+03	-8.42E+03	-1.17E+04	6.74E+03
	c_1	-2.19E+02	5.40E+02	5.55E+02	5.92E+02	2.82E+02
	c_0	6.45E-01	1.17E-01	-1.45E+00	1.28E+06	5.49E+00
S.5	c_5	8.18E+07	-1.60E+07	7.83E+06	-5.00E+05	-2.13E+04
	c_4	-8.05E+06	3.89E+06	-1.66E+06	3.04E+05	2.73E+04
	c_3	1.15E+05	-3.07E+05	5.04E+04	-6.14E+04	-1.21E+04
	c_2	-1.87E+03	3.52E+03	4.87E+03	3.78E+03	1.97E+03
	c_1	8.95E+02	8.11E+02	2.90E+02	3.50E+02	4.76E+01
	c_0	4.19E+00	5.45E+00	1.24E+01	4.77E+00	8.83E-01

The fitting coefficients (c_0, c_1, c_2, c_3, c_4, c_5) for fitting the airflow with fSampEn of EMGdi for each subject under 5 different breathing states are different.

inspiratory airflow. For all subjects, the mean correlation coefficient value in any breathing state is above 0.8013, and the average value is 0.8133 for a very strong correlation. Like the $EMGdi_e$, the time series fSampEn of EMGdi has a strong correlation with the inspiratory airflow, the smallest mean value is 0.8003, and the largest value reaches 0.8614 for a very strong correlation. Mean correlation between fSampEn and inspiratory airflow for each subject in all breathing states reached 0.8325 for a very strong correlation. The result shows that we use time series fSampEn to verify the feasibility of the inspiratory airflow. All correlations are statistically significant ($p < 0.001$).

Fig. 5 illustrates the comparison between predicted airflow by multiple fitting coefficients (red dotted line) and a fitting coefficient (purple dotted line) and actual airflow (green solid line) of 5 subjects in 5 breathing state (Quiet breathing, Forced breathing I, Forced breathing II, Forced breathing III and Forced breathing IV) based on polynomial curve fitting method and nonlinear programming method using time series fSampEn of EMGdi. It was found that the predicted airflow curve (red dotted line) of inhalation in a breathing cycle by different fitting coefficients at different breathing state fits the actual airflow (green solid line) better, and all the values of coefficient of determination (R_1^2) are greater than 0.8913. The R_1^2 do not change with changes in the respiratory airflow amplitude and inspiratory time caused by the increase in the degree of inhalation effort. It was observed that the polynomial regression analysis method used to establish the correlation

TABLE V
A COEFFICIENT TO FIT AIRFLOW BASED ON FSAMPEN FOR EACH SUBJECT IN 5 SUBJECTS IN FIG.5

Breathing state		c_5	c_4	c_3	c_2	c_1	c_0
S.1	B1-B5	-6.65E+04	1.26E+05	-6.19E+04	9.93E+03	6.08E+01	-2.24E+00
S.2	B1-B5	8.68E+04	1.32E+05	-8.61E+04	1.33E+04	-1.10E+02	7.24E+00
S.3	B1-B5	3.66E+04	1.26E+05	-7.48E+04	1.16E+04	1.39E+02	-1.93E+00
S.4	B1-B5	5.43E+04	6.31E+04	-5.07E+04	9.19E+03	-4.76E+00	7.60E-01
S.5	B1-B5	-2.51E+05	2.56E+05	-8.91E+04	1.13E+04	1.17E+01	4.88E-01

B1-B5 represent 5 breathing states for each subject (B1: Quiet breathing, B2: Forced Breathing Ⅰ, B3: Forced Breathing Ⅱ, B4: Forced Breathing Ⅲ, B5: Forced Breathing Ⅳ). The fitting coefficients (c_0, c_1, c_2, c_3, c_4, c_5) for fitting the airflow with fSampEn of EMGdi for each subject under 5 different breathing states are same.

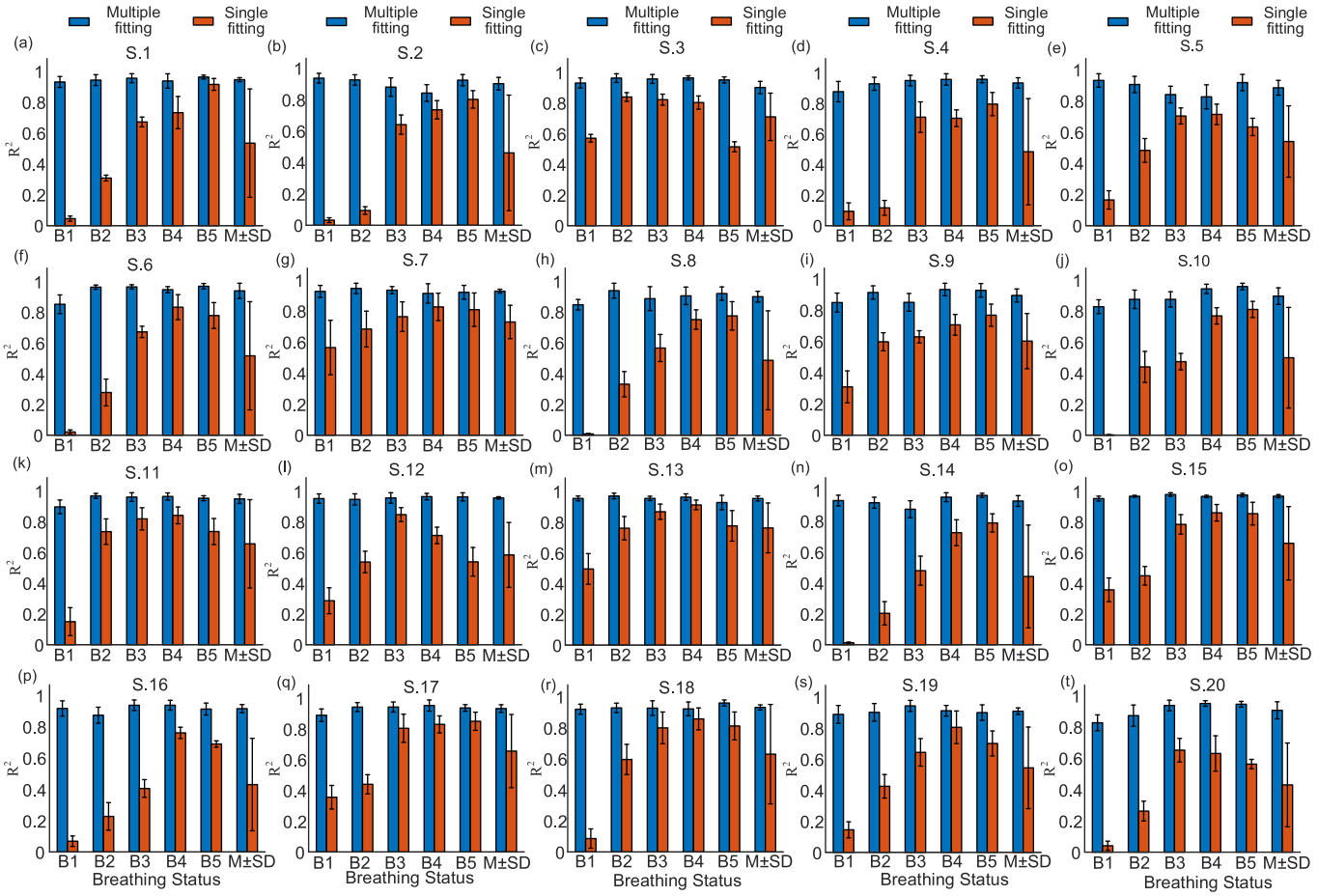

Fig. 6. Coefficients of determination (R^2) between predicted inspiratory airflow and actual inspiratory airflow in 20 subjects using multiple fitting coefficients and a coefficient for their 15 consecutive inspiratory airflows. M ± SD: mean ± standard deviation.

of fSampEn of EMGdi and the airflow is reliable and feasible.

Nonlinear programming method was used to solve a fitting coefficient for each subject at 5 different breathing state. The different degrees of overall decline in R_2^2 in 5 subjects was found. Compared with the goodness of fit of the other four subjects, S.4 has the best goodness of fit with average R_2^2 for 0.8755. Using a fitting coefficient to fit airflow cannot make the goodness of fit in all breathing states reach the best, but it can make R_2^2 reach the local optimum. It means that using a fitting coefficient for each subject can simultaneously make two or more of the five breathing states achieve a good fitting effect ($R^2 > 0.7$), such as S.2 for 0.9653 and 0.8722 in Forced breathing II and Forced breathing III respectively. Although R_2^2 of the Quiet breathing state in Fig.5 is smaller than the other four breathing states, the predicted airflow waveform (purple dotted line) change can maintain the same trend as the actual airflow change.

Table IV shows multiple fitting coefficients for 5 subjects in different breathing state to fit the actual inspiratory airflow based on the polynomial regression analysis method using fSampEn of the EMGdi as a characteristic parameter. These coefficients seem to be different intuitively, but the fitting coefficient values of each subject in the same breathing state

have a certain degree of similarity, such as exponent of c_5 for 8 of S.1 and S.2 in Quiet breathing state. The difference in fitting coefficient values and airflow values between Quiet breathing state and Forced breathing IV state are great.

Table V explains a coefficient based on the nonlinear programming method to fit the airflow in all breathing states for each subject in 5 subjects (Fig.5). The fitting coefficients of 5 subjects are different, which also have a certain degree of similarity, such as exponent of c_5 for 4 of S.1, S.2, S.3 and S.4.

Fig. 6 indicates the comparison of the R^2 for all subjects based on different coefficients and a single coefficient for each subject in 5 breathing states. The R^2 in Fig. 6 is mean $\pm$ standard deviation (M $\pm$ SD) of R^2 of each subject's 15 consecutive inspiratory airflow under 5 different breathing conditions. The minimum R^2 value is 0.8282 ± 0.0772, and the maximum achieves 0.9788 ± 0.0116 by different fitting coefficients for each subject. The M $\pm$ SD of R^2 of each subject in different breathing states reached more than 0.8862 ± 0.0476 by different fitting coefficients. The above results show that fitting the respiratory airflow curve using polynomial regression analysis method with the time series fSampEn has good adaptability for all subjects. A coefficient for each subject to fit the airflow in different breathing states decreases R^2 for all subjects. The minimum R^2 value is 0.0023 ± 0.0017, and the maximum achieves 0.9159 ± 0.0384 by different fitting coefficients in all subjects. The change trend of R^2 of all subjects in Fig. 6 under different breathing states is the same as Fig. 5. On the whole, the R^2 in quiet breathing state is smaller than the other four breathing states. The M $\pm$ SD of R^2 of each subject by a fitting coefficient in different breathing states was between 0.4298 ± 0.2677 and 0.7622 ± 0.1619.

IV. Discussion and Conclusion

In respiratory health monitoring, clinical diagnosis and rehabilitation training, the respiratory function is usually evaluated based on intuitive respiratory airflow, but this method requires wearing a tight mask or clamp the nose during the monitoring process. It is well known that the respiratory function is correlated with EMGdi [7], [35]. The collection of EMGdi is more comfortable and cheaper compared to airflow. However, the EMGdi is affected by the ECG signal and cannot be filtered directly by setting a simple filter, affecting the evaluation of correlation between EMGdi and airflow. A quantification method of EMGdi that is not sensitive to ECG interference called fSampEn has been proposed in some studies [18], [19], [24]. However, it was not found in the literature that researchers compare and analyze the EMGdi before and after filtering to verify the reliability of the fSampEn method.

In this paper, a combination of QRS positioning and stationary wavelet transform was used to filter out ECG interference in EMGdi. The fSampEn and RMS of EMGdi and $EMGdi_p$ in the 1-s moving window were calculated in a state of increasing forceful breathing. Consistent with previous research, fSampEn and RMS of EMGdi increase with the increase in the degree of exertion [18], [24], [36], which is mainly reflected in the increase in the degree of breathing effort making the EMGdi action potential superimposed more densely. Then influence of the ECG on EMGdi was analyzed by calculating the correlation between the time series fSampEn and the RMS of EMGdi before and after the filter. By comparing and analyzing spearman's correlation coefficient (ρ) and mean squared error (MSE) for fSampEn and RMS of the EMGdi before and after filtering in Fig.4, we found that the fSampEn is more robust to ECG interference than the RMS. The fSampEn after the ECG is filtered has a significant change in amplitude compared with that before the filtering, but the time series waveform does not change significantly. In order to further illustrate the consistency between the time series fSampEn and the amplitude change of EMGdi, we analyzed the correlation between the fSampEn of EMGdi (or $EMGdi_p$) and $EMGdi_e$ in Table I. The correlation between fSampEn and $EMGdi_e$ do not change significantly with the filtering of the ECG. Before predicting the airflow, we proposed to analyze the correlation between fSampEn of the EMGdi and the $EMGdi_e$, and found the correlation between the two with no significant difference. The strong correlation between the airflow signal and fSampEn of the EMGdi illustrated the feasibility of using time series fSampEn to predict respiratory airflow.

In previous study [7], it was proposed to use the envelope of EMGdi to estimate airflow, but the ECG interference in the EMGdi must be filtered out. However, the process of filtering out the ECG signal is cumbersome and complicated, increasing the difficulty of predicting airflow. Regression analysis has been used to describe the quantitative relationship between surface EMG and muscle strength [37], [38]. In this paper, under the premise of fully demonstrating that the time series of fSampEn was not sensitive to the ECG, and had a strong correlation with the amplitude (envelope) of EMGdi and the airflow, a method for predicting respiratory airflow using time series fSampEn of EMGdi based on polynomial regression analysis was firstly proposed. The fitting effect R^2 (Fig. 5) show that in any breathing state, the polynomial regression analysis method predicts inspiratory airflow is applicable to all subjects. Using time series fSampEn of EMGdi as the characteristic parameter to evaluate the respiratory airflow does not need to filter out the ECG, which is simple, reliable and convenient.

We adjusted the fitting coefficient between fSampEn of EMGdi and airflow for each subject in each breathing state (Table IV, Fig. 6). Intuitively, these coefficients were various. However, there was a certain similarity in the order of magnitude in same breathing state for each subject. It is ideal and more meaningful for a subject to fit the airflow in different breathing state with the same coefficient using fSampEn of EMGdi. A fitting coefficient for a subject was solved based on nonlinear programming method (Table V, Fig. 6). Fig. 5 illustrates the results of fitting the airflow with a coefficient for each subject. It was found that the R^2 dropped overall in 5 subjects. The effect of fitting the airflow using fSampEn of EMGdi with a coefficient in any breathing state among different subject was different. R^2 of S.4 was higher than that of other four subjects on the whole. However, a coefficient for each subject that could make the fitting effect reach the local optimum, such as S.2 in Forced Breathing II and Forced Breathing III. A fitting coefficient that made R^2 for each

subject in any breathing state reach above 0.7 wasn't obtained, which was due to great difference in fitting coefficient values and airflow values between Quiet breathing state and Forced IV breathing state. Nevertheless, it is feasible to calculate a fitting coefficient for a subject within a certain range of airflow and achieve good R^2 for local optimum in Fig. 5. The airflow range value need to be mined in future research work. It is meaningful to predict airflow based on fSampEn of EMGdi within a certain range in a specific application scenarios. In existing mechanical ventilation with ventilators, the tidal volume integrated by airflow is usually set within 10-15ml/kg without causing damage to the patient's lungs [39]. The triggering and control of the traditional ventilator is based on artificially set airflow waveform and trigger time, which does not meet physiological needs of human and easily cause emergence of man-machine asynchronous [40]. Using fSampEn EMGdi to predict the respiratory airflow that meets the physiological needs of the human within a certain range of airflow values is of great significance to the optimization of traditional ventilators. It also optimizes the complicated operation and expensive status of the esophageal electrode detecting EMGdi to control ventilator [7], [40]. When the algorithm for predicting airflow based on EMGdi is used in an airflow detection instrument, it can be used to detect the amplitude of fSampEn of EMGdi to distinguish different inhalation modes and then calculate the airflow. It improves the discomfort and inconvenience caused by the nasal prongs, mask and thermistor to detect the airflow [40].

Although a quantitative relationship between EMGdi and airflow has been established and the potential for using fSampEn of EMGdi to predict airflow has been evaluated, we acknowledge that there are some limitations in our research that need to be investigated to further improve our work. Firstly, fixed ventilation pattern based on visual feedback to control the respiratory rate and airflow peak was used to establish the relationship between EMGdi and airflow. These results need to be confirmed in uncontrolled and variable ventilatory patterns. Secondly, the participants in our experiment were 20 young healthy adults without respiratory diseases. Measurement of EMGdi and airflow of older subjects and comparing them with the results of young subjects should be the focus of future research. Future work should also investigate the reproducibility of correlation results of EMGdi and airflow in patients with impaired respiratory neuromechanical efficiency. Finally, data mining technology such as neural networks, association rules and classification methods should be applied to explore the implicit, regular and unknown connection between fSampEn of EMGdi and airflow signals among subjects in health and disease.

REFERENCES

[1] A. N. Norali, A. H. Abdullah, Z. Zakaria, N. A. Rahim, and S. K. Nataraj, "Human breathing classification using electromyography signal with features based on Mel-frequency cepstral coefficients," *Int. J. Integr. Eng.*, vol. 9, no. 4, pp. 85–92, Dec. 2017.

[2] J. Park, J. Lee, J. Yang, B. Lee, and D. Han, "Effects of combined exercise on changes of lower extremity muscle activation during walking in older women," *J. Phys. Therapy Sci.*, vol. 27, no. 5, pp. 1515–1518, 2015.

[3] M. Sin *et al.*, "Electromyographic analysis of upper limb muscles during standardized isotonic and isokinetic robotic exercise of spastic elbow in patients with stroke," *J. Electromyogr. Kinesiol.*, vol. 24, no. 1, pp. 11–17, Feb. 2014.

[4] O. L. Wade, "Movements of the thoracic cage and diaphragm in respiration," *J. Physiol.*, vol. 124, no. 2, pp. 193–212, May 1954.

[5] C. J. Jolley *et al.*, "Neural respiratory drive in healthy subjects and in COPD," *Eur. Respiratory J.*, vol. 33, no. 2, pp. 289–297, Sep. 2008.

[6] L. Lin, L. Guan, W. Wu, and R. Chen, "Correlation of surface respiratory electromyography with esophageal diaphragm electromyography," *Respiratory Physiol. Neurobiol.*, vol. 259, pp. 45–52, Jan. 2019.

[7] G. Biagetti, P. Crippa, L. Falaschetti, and C. Turchetti, "Correlation between respiratory action and diaphragm surface EMG signal," in *Proc. 41st Eng. Med. Biol. (EMB) Conf.*, 2019, pp. 33–46.

[8] De Luca and J. Carlo, "Surface electromyography: Detecting and recording," *DelSys Incorporated*, vol. 10, no. 2, pp. 1–10, 2002.

[9] C. Sinderby, L. Lindström, and A. E. Grassino, "Automatic assessment of electromyogram quality," *J. Appl. Physiol.*, vol. 79, no. 5, pp. 1803–1815, Nov. 1995.

[10] C. Sinderby, S. Friberg, N. Comtois, and A. Grassino, "Chest wall muscle cross talk in canine costal diaphragm electromyogram," *J. Appl. Physiol.*, vol. 81, no. 5, pp. 2312–2327, Nov. 1996.

[11] G. Luo, P. Qiu, W. Huang, and L. Huang, "Applying stationary wavelet transform for locating and cancelling electrocardiogram interference interval in diaphragmatic electromyography," in *Proc. IEEE Symp. Product Compliance Eng.-Asia (ISPCE-CN)*, Dec. 2018, pp. 1–5.

[12] J. Beck, C. Sinderby, L. Lindström, and A. Grassino, "Diaphragm interference pattern EMG and compound muscle action potentials: Effects of chest wall configuration," *J. Appl. Physiol.*, vol. 82, no. 2, pp. 520–530, Feb. 1997.

[13] M. Ungureanu, G. Staude, and W. Wolf, "Comparative study of event-synchronous interference cancelling methods," in *Proc. Int. Conf. IEEE Eng. Med. Biol. Soc.* New York, NY, USA: IEEE.

[14] P. Akkiraju and D. C. Reddy, "Adaptive cancellation technique in processing myoelectric activity of respiratory muscles," *IEEE Trans. Biomed. Eng.*, vol. 39, no. 6, pp. 652–655, Jun. 1992.

[15] Y. Deng, W. Wolf, R. Schnell, and U. Appel, "New aspects to event-synchronous cancellation of ECG interference: An application of the method in diaphragmatic EMG signals," *IEEE Trans. Biomed. Eng.*, vol. 47, no. 9, pp. 1177–1184, Sep. 2000.

[16] Y. Lu, Y. Xian, J. Chen, and Z. Zheng, "A comparative study to extract the diaphragmatic electromyogram signal," in *Proc. Int. Conf. Biomed. Eng. Informat.*, Sanya, China, May 2008, pp. 315–319.

[17] V. von Tscharner, B. Eskofier, and P. Federolf, "Removal of the electrocardiogram signal from surface EMG recordings using non-linearly scaled wavelets," *J. Electromyography Kinesiol.*, vol. 21, no. 4, pp. 683–688, Aug. 2011.

[18] L. Estrada, A. Torres, L. Sarlabous, and R. Jane, "Improvement in neural respiratory drive estimation from diaphragm electromyographic signals using fixed sample entropy," *IEEE J. Biomed. Health Informat.*, vol. 20, no. 2, pp. 476–485, Mar. 2016.

[19] M. Lozano-García *et al.*, "Surface mechanomyography and electromyography provide non-invasive indices of inspiratory muscle force and activation in healthy subjects," *Sci. Rep.*, vol. 8, no. 1, pp. 1–13, Nov. 2018.

[20] J. S. Richman and J. R. Moorman, "Physiological time-series analysis using approximate entropy and sample entropy," *Amer. J. Physiol.-Heart Circulatory Physiol.*, vol. 278, no. 6, pp. 2039–2049, 2000.

[21] H. Nakano *et al.*, "Validation of a single-channel airflow monitor for screening of sleep-disordered breathing," *Eur. Respiratory J.*, vol. 32, no. 4, pp. 1060–1067, May 2008.

[22] C. S. Sassoon, "Triggering of the ventilator in patient-ventilator interactions," *Respiratory Care*, vol. 56, no. 1, pp. 39–51, Jan. 2011.

[23] F. Q. Al-Khalidi, R. Saatchi, D. Burke, H. Elphick, and S. Tan, "Respiration rate monitoring methods: A review," *Pediatric Pulmonol.*, vol. 46, no. 6, pp. 523–529, Jun. 2011.

[24] L. Estrada, A. Torres, L. Sarlabous, and R. Jane, "Onset and offset estimation of the neural inspiratory time in surface diaphragm electromyography: A pilot study in healthy subjects," *IEEE J. Biomed. Health Informat.*, vol. 22, no. 1, pp. 67–76, Jan. 2018.

[25] M. Schmidt, B. Foitzik, R. R. Wauer, F. Winkler, and G. Schmalisch, "Comparative investigations of algorithms for the detection of breaths in newborns with disturbed respiratory signals," *Comput. Biomed. Res.*, vol. 31, no. 6, pp. 413–425, Dec. 1998.

[26] Y. J. Xie, Z. Yang, Z. P. Fan, and Y. M. Luo, "Application of wavelet to the cancellation of ECG interference in diaphragmatic EMG," *Acta Electronica Sinica*, vol. 38, no. 2, pp. 360–370. Jun. 2010.
[27] Z. Yang, G. Luo, and F. F. Yuan, "Wavelet tansform in electromyography of diaphragm denoising," *J. Data Acquisition Process.*, vol. 28, no. 5, pp. 546–552, Jan. 2013.
[28] D. L. Donoho, A. Maleki, and A. Montanari, "Message passing algorithms for compressed sensing: II. Analysis and validation," in *Proc. IEEE Inf. Theory Workshop (ITW)*, Cairo, Egypt, Jan. 2010, pp. 1–5.
[29] G. Luo and Z. Yang, "The application of ECG cancellation in diaphragmatic electromyographic by using stationary wavelet transform," *Biomed. Eng. Lett.*, vol. 8, no. 3, pp. 259–266, Apr. 2018.
[30] L. Sarlabous, A. Torres, J. A. Fiz, and R. Jané, "Evidence towards improved estimation of respiratory muscle effort from diaphragm mechanomyographic signals with cardiac vibration interference using sample entropy with fixed tolerance values," *PLoS ONE*, vol. 9, no. 2, pp. 1–9, Feb. 2014.
[31] I. Campanini, A. Merlo, P. Degola, R. Merletti, G. Vezzosi, and D. Farina, "Effect of electrode location on EMG signal envelope in leg muscles during gait," *J. Electromyogr. Kinesiol.*, vol. 17, pp. 515–526, Aug. 2007.
[32] D. Špulák, R. Čmejla, P. Mikulíková, P. J. Bezoušková, and B. Kračmar, "Muscle activity detection using EMG envelope thresholding-comparison of various approaches," in *Proc. 20th Annu. Conf. Proc. Tech. Comput.*, Bratislava, Slovakia, 2012, pp. 1–5.
[33] M. Du, B. Hu, and F. Xiao, "Detection of stretch reflex onset based on empirical mode decomposition and modified sample entropy," *BMC Biomed. Eng.*, vol. 1, no. 1, pp. 1–10, Sep. 2019.
[34] J. D. Evans, *Straightforward Statistics for the Behavioral Sciences*. Boston, MA, USA: Thomson Brooks, 1996.
[35] G. J. Hutten, L. A. van Eykern, P. Latzin, M. Kyburz, W. M. van Aalderen, and U. Frey, "Relative impact of respiratory muscle activity on tidal flow and end expiratory volume in healthy neonates," *Pediatric Pulmonol.*, vol. 43, no. 9, pp. 882–891, Sep. 2008.
[36] J. W. Chow and D. S. Stokic, "Variability, frequency composition, and complexity of submaximal isometric knee extension force from subacute to chronic stroke," *Neuroscience*, vol. 273, pp. 189–198, Jul. 2014.
[37] S. Boe, C. Rice, and T. Doherty, "Estimating contraction level using root mean square amplitude in control subjects and patients with neuromuscular disorders," *Arch. Phys. Med. Rehabil.*, vol. 89, pp. 711–718, Apr. 2008.
[38] J. H. Lawrence and C. J. De Luca, "Myoelectric signal versus force relationship in different human muscles," *J. Appl. Physiol.*, vol. 54, no. 6, pp. 1653–1659, 1983.
[39] M. J. Tobin, "Advances in mechanical ventilation," *New England J. Med.*, vol. 344, no. 26, pp. 1986–1996, 2001.
[40] P. Navalesi, D. Colombo, and F. D. Corte, "NAVA ventilation," *Minerva Anestesiol*, vol. 76, no. 5, pp. 346–352, Mar. 2010.